

# The structure and magnetism of graphone

*L. Feng, W. X. Zhang\**

Computational Condensed Matter Physics Laboratory, Department of Physics, Taiyuan  
University of Technology, Taiyuan 030024, People's Republic of China

Graphone is half-hydrogenated graphene. The structure of graphone is illustrated as trigonal adsorption of hydrogen atoms at first. However, we found the trigonal adsorption is metastable. We present an illustration in detail to explain how a trigonal adsorption geometry evolves into a rectangular adsorption geometry. We check the change of magnetism during the evolution of geometry by evaluating the spin polarization of the intermediate geometries. We prove and clarify that the rectangular adsorption of hydrogen atoms is the most stable geometry of graphone and graphone is actually antiferromagnetic.

Graphene, a single atomic layer of carbon atoms, is a great candidate for engineering electronic devices of atomic thickness.<sup>1-3</sup> With band crossing at the Dirac points of the Brillouin zone, the pristine graphene is a semimetal and its conducting properties are remarkable.<sup>4,5</sup> In order to apply graphene into electronics and photonics,<sup>6</sup> a great interest on graphene with a tunable band gap in the intermediate energy range is stimulated. So far, these gap-opening strategies can be classified into two basic mechanisms: one is to disrupt the band crossing at the Dirac points by breaking the balance of the two sublattices of graphene; two is to make the carbon hybridization transform from  $sp^2$  to  $sp^3$  by chemical functionalization. Chemical functionalization<sup>7-9</sup> is a useful tool to tune the band structure<sup>1,10</sup> and majority carrier type of

materials for electronic and optical applications.<sup>11-14</sup> It has been experimentally demonstrated<sup>7</sup> that a band gap can be introduced in the highly conducting semimetallic graphene with chemisorption of atomic hydrogen.<sup>15</sup> J. Zhou et al. has investigated semihydrogenated graphene sheet which is referred to as graphone with the configuration shown in Fig. 1.<sup>16</sup> Their calculations indicate that the unhydrogenated carbon atoms couple ferromagnetically and the system is semiconducting. Based on the geometry in Fig. 1 (We name it as triangular graphone), we make geometry optimization and find that the stable structure should be the geometry in Fig. 2. We name it as rectangular graphone. The electronic structure calculation indicates that rectangular graphone is antiferromagnetic and is an indirect band gap semiconductor with a 2.5eV band gap, very different from the triangular graphone (ferromagnetic and with a smallband gap).

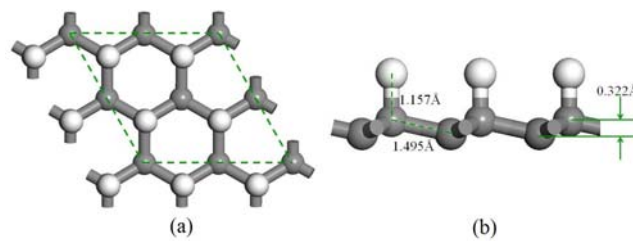


Figure 1. Trigangular geometry of graphone. (a) Top view with the green rhombus shows the unit cell, (b) Side view shows C-C and C-H distances.

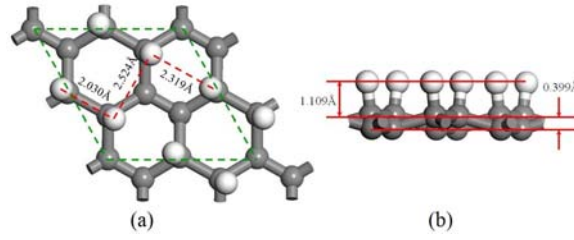


Figure 2. Rectangular geometry of graphone. (a) Top view with the green rhombus shows the unit cell and red lines shows the distances between H atoms, (b) Side view shows distance between C and H planes.

Our first-principle calculations are based on spin-polarized density functional theory (DFT) with generalized gradient approximation (GGA) using Perdew-Burke-Ernzerhof (PBE) exchange correlation potential and the ultrasoft pseudopotential. We use the geometry in Reference 16 which consisting of eight carbon atoms and four hydrogen atoms shown in Fig. 1. The bond lengths of C-C and C-H are 1.495 and 1.157 Å, respectively. The distance between two C planes is 0.322 Å. To avoid interactions between two cells, vacuum space is set as 15Å. The k-points in reciprocal space is set as  $7 \times 7 \times 1$ , following the Monkhorst–Pack scheme. The structure is relaxed with a cutoff energy of 310eV. No symmetry constraints are used. The convergence of energy and force are set as  $1 \times 10^{-4}$ eV and 0.01eV/Å, respectively.

The stable geometry is shown in Fig. 2. The bond length of C-H is 1.133 Å, smaller than that of triangular geometry. Different from triangular geometry, the bond of C-H is not perpendicular to C planes. All the H atoms are still in the same plane. The distance between the H atoms are 2.030, 2.524 and 2.319 Å, respectively. The distance between two C planes is 0.399 Å. This distance is a little larger than that of triangular graphone. The distance between C and H planes is 1.109 Å. Hornekaer L. et al. has investigated the topograph of hydrogenated graphene by STM.<sup>17</sup> Both Dimmer A and Dimmer B are part of the rectangular geometry we obtained here. In the STM image they obtained, we could not find the structure corresponding to triangular

graphone. This is a powerful proof for the conclusion that the rectangular graphone is stable while the triangular graphone is metastable.

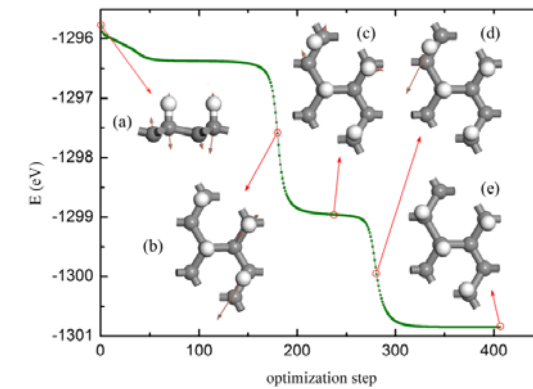


Figure 3. Dependence of energy on optimization step. Geometry and diagrammatic sketches of the forces for the corresponding step: (a)  $n=1$  (triangular graphone), (b)  $n=175$ , (c)  $n=240$ , (d)  $n=278$  and (e)  $n=417$  (rectangular graphone).

The dependence of energy on optimization step is shown in Fig. 3. The evolution of geometry takes 417 steps. The insets are the geometry and diagrammatic sketches of the force for corresponding step,  $n=1$ , 175, 278 and 417. The inset (a) in Fig. 3 shows that the force on C and H atoms of triangular graphone is perpendicular to the C and H plane. The inset (b) in Fig. 3 shows the intermediate geometry corresponding to the drastic decrease of energy. Two H atoms has deviated its original sites. The Force on one of the two H atoms is considerable. It can be induced that the triangular graphone is metastable. This means that, once a perturbation along the C/H plane is exerted in triangular graphone, the H atoms tend to move away from their original sites. The total energy decreases dramatically with H atom moving and H atom would jump to the top site above the C atom which the force directs to. After the jump of H atom, the

configuration reaches to another metastable state and the energy line stays at a platform. This metastable geometry is depicted in the inset (c) in Fig. 3. One H atom has been on the stable position and the other H atom deviates its original position partially. There are no forces on H atoms. The forces on the C atoms are small and parallel to the C/H plane. The inset (d) in Fig. 3 shows the geometry corresponding to the second energy decrease. There is a large force exerting on the H atom with partially deviation. It can be induced that the second H atom would move to the top site above C atom which the force directs to. After the jump of second H atom, the geometry reaches to the stable state, rectangular graphone. Its diagrammatic sketch of the force is shown in the inset (e) in Fig. 3. The forces exerting on C and H atoms are almost zero.

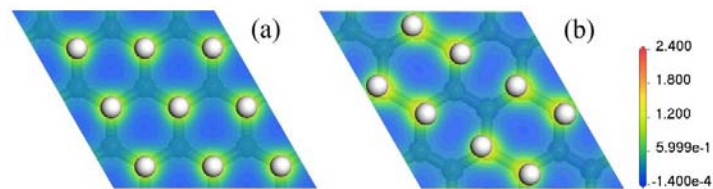


Figure. 4 Calculated electron density of (a) triangular graphone and (b) rectangular graphone. Both of the slices are located in the middle of C plane and H plane. The unit is  $e/\text{\AA}^3$ .

To understand the change of electronic interaction, electronic densities for the two geometries are plotted in Fig. 4. Both of the slices are located in the middle of C and H planes. We can find that in triangular graphone the electrons are localized in the hydrogen atoms. There are almost no electrons in the space between hydrogen atoms. It means that the interaction between H atoms is very weakly in triangular graphone. It is the reason why the triangular graphone is metastable. While in rectangular graphone, the electrons are no longer localized in H atoms. The electron density in the space between H atoms is considerable. It indicates that the interaction between H atoms is enhanced in rectangular graphone. That is why its total energy is lower than triangular graphone.

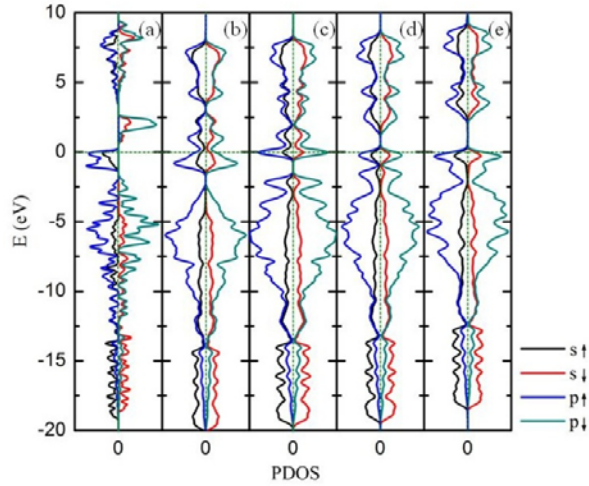


Figure. 5 Calculated PDOS of the corresponding geometry for (a)  $n=1$  (triangular graphone), (b)  $n=175$ , (c)  $n=240$ , (d)  $n=278$  and (e)  $n=417$  (rectangular graphone) with black curve representing spin up s-electrons, red the spin down s-electrons, blue the spin up p-electrons, and cyan the spin down p-electrons.

Since the triangular graphone is not a stable geometry, it is not possible to introduce magnetism by constructing this geometry in practice. What we are interested in is whether rectangular graphone is magnetic. Fig. 5 shows the calculated PDOS of the five representative structures. Besides the triangular graphone in which a clear magnetic splitting is observed, the net moments for other structures are zero, indicating that the rectangular graphone is antiferromagnetic. It means that it is not possible to introduce ferromagnetism into graphene by semi-hydrogenating.

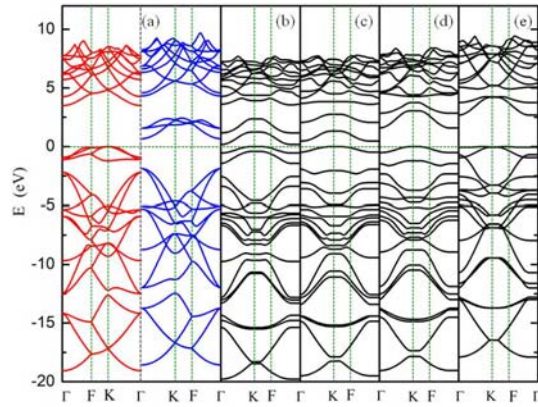


Figure 6. Calculated band structures of the corresponding geometry for (a)  $n=1$  (triangular graphone), (b)  $n=175$ , (c)  $n=240$ , (d)  $n=278$  and (e)  $n=417$  (rectangular graphone).  $G=(0, 0, 0)$ ,  $K=(-1/3, 2/3, 0)$  and  $F=(0, 1/2, 0)$ .  $G$  presents the  $\Gamma$  point and  $K$  is the Dirac point of graphene.

To understand the properties of rectangular graphone further, the band structures for the five representative geometries are calculated and depicted in Fig. 6. Examination of the states near the Fermi level shows that the two doping state above the Fermi level shifts to the high energy region while the two doping state below the Fermi level shifts to the low energy region, resulting in a energy gap of about 2.5eV, which is smaller than that of graphane.<sup>18</sup> The rectangular graphone is an indirect bandgap semiconductor with valence band maximum located at the  $K$  point and conduction band minimum at the  $G$  point. This conclusion is consistent with the calculation carried out by Samarakoon D. K. et al.<sup>19</sup>

In conclusion, by density functional theory we have investigated the structure and magnetism of graphone. Based on the triangular graphone, the geometry optimization has been performed. It can be found that the triangulare graphone is metastable. In the optimization process, there are two typical physical processes which are corresponding to two energy

decreases. The two processes are that two H atoms move to the neighboring C atoms one after another, forming the typical geometry of rectangular graphone. Comparison of the electron density of triangular graphone with that of rectangular graphone indicates that the interaction between H atoms is enhanced in rectangular graphone, which proves again that the rectangular graphone is a more stable structure than triangular graphone. The electronic structure calculation indicates that, different from the triangular graphone a ferromagnetic semiconductor with a small indirect band gap, the rectangular graphone is an antiferromagnetic semiconductor with an indirect band gap of about 2.5eV. These findings above indicate that magnetism cannot be introduced by semi-hydrogenating graphene.

\*To whom correspondence should be addressed: zhangwenxing@tyut.edu.cn

#### ACKNOWLEDGMENT

This work is supported by the National Natural Science Foundation of China in Grant No.xxx.

#### REFERENCES

- (1) Novoselov, K. S.; Geim, A. K.; Morozov, S. V.; Jiang, D.; Zhang, Y.; Dubonos, S. V.; Grigorieva, I. V.; Firsov, A. A. *Science* 2004, 306, 666-669.
- (2) Gass, M. H.; Bangert, U.; Bleloch, A. L.; Wang, P.; Nair, R. R.; Geim, A. K. *Nat. Nanotech.* 2008, 3, 676-681.
- (3) Stankovich, S.; Dikin, D. A.; Dommett, G. H. B.; Kohlhaas, K. M.; Zimney, E. J.; Stach, E. A.; Piner, R. D.; Nguyen, S. T.; Ruoff, R. S. *Nat. Lett.* 2006, 442, 282-286.
- (4) Geim, A. K. *Science* 2009, 324, 1530-1534.
- (5) Katsnelson, M. I. *Mater. Today* 2007, 10, 20-27.

- (6) Novoselov, K. Nat. Mater. 2007, 6, 720-721.
- (7) Elias, D. C.; Nair, R. R.; Mohiuddin, T. M. G.; Morozov, S. V.; Blake, P.; Halsall, M. P.; Ferrari, A. C.; Boukhvalov, D. W.; Katsnelson, M. I.; Geim, A. K.; Novoselov, K. S. Science 2009, 323, 610–613.
- (8) Robinson, J. T.; Burgess, J. S.; Junkermeier, C. E.; Badescu, S. C.; Reinecke, T. L.; Perkins, F. K.; Zalalutdinov, M. K.; Baldwin, J. W.; Culbertson, J. C.; Sheehan, P. E.; Snow, E. S. Nano Lett. 2010, 10, 3001–3005.
- (9) Englert, J. M.; Dotzer, C.; Yang, G.; Schmid, M.; Papp, C.; Gottfried, J. M.; Steinrueck, H.-P.; Spiecker, E.; Hauke, F.; Hirsch, A. Nat. Chem. 2011, 3, 279–286.
- (10) Zhang, Y. B.; Tan, Y. W.; Stormer, H. L.; Kim, P. Nature 2005, 438, 201–204.
- (11) Gao, H. L.; Wang, L.; Zhao, J. J.; Ding, F.; Lu, J. P. J. Phys. Chem. C 2011, 115, 3236–3242.
- (12) Haberer, D.; Vyalikh, D. V.; Taioli, S.; Dora, B.; Farjam, M.; Fink, J.; Marchenko, D.; Pichler, T.; Ziegler, K.; Simonucci, S.; Dresselhaus, M. S.; Knupfer M.; Buchner, B.; Gruneis, A. Nano Lett. 2010, 10, 3360–3366.
- (13) Jeon, K.-J.; Lee, Z.; Pollak, E.; Moreschini, L.; Bostwick, A.; Park, C.-M.; Mendelsberg, R.; Radmilovic, V.; Kostecky, R.; Richardson, T. J.; Rotenberg, E. ACS Nano 2011, 5, 1042–1046.
- (14) Cheng, S.-H.; Zou, K.; Okino, F.; Gutierrez, H. R.; Gupta, A.; Shen, N.; Eklund, P. C.; Sofo, J. O.; Zhu, J. Phys. Rev. B 2010, 81, 205435.

- (15) Sofo, J. O.; Chaudhari, A. S.; Barber, G. D. *Phys. Rev. B: Condens. Matter Mater. Phys.* 2007, 75, 153401-1–153401-4.
- (16) Zhou, J.; Wang, Q.; Sun, Q.; Chen, X. S. Kawazoe, Y.; Jena, P. *Nano lett.* 2009, 9, 3867–3870
- (17) Hornekaer, L.; Sljivancanin, Z.; Xu, W.; Otero, R.; Rauls, E.; Stensgaard, I.; Laegsgaard, E.; Hammer, B.; Besenbacher, F. *Phys. Rev. Lett.* 2006, 96, 156104-1–156104-4.
- (18) Topsakal, M.; Cahangirov, S.; Ciraci, S. *Appl. Phys. Lett.* 2010, 96, 091912-1–091912-3.
- (19) Samarakoon, D. K.; Wang, X. Q. *ACS Nano*, 2009, 3, 4017–4022